THE JOURNAL OF PROSTHETIC DENTISTRY

RESEARCH AND EDUCATION

Adhesion of *Streptococcus mutans* on highly translucent zirconia: Influence of surface properties and polyelectrolyte multilayer coatings

Anže Abram, PhD,[a] Lana Staver, MSc,[b] Franc Rojko, MSc,[c] Roman Štukelj, PhD,[d] Tin Klačić, PhD,[e] Davor Kovačević, PhD,[f] Anamarija Zore, PhD,[g] and Klemen Bohinc, PhD[h]

ABSTRACT

Statement of problem. Low-pressure airborne-particle abrasion has been used to improve the adhesion of zirconia to resin cement. However, whether a polyelectrolyte multilayer can be used to reduce bacterial adhesion to abraded zirconia is unclear.

Purpose. The purpose of this in vitro study was to evaluate whether polyelectrolyte multilayers added to airborne-particle abraded zirconia can minimize biofilm development.

Material and methods. Commercially available zirconia powders with yttria content between 3 and 5 mol% were isostatically pressed into Ø20-mm disks and sintered at 1450 °C for 2 hours (n=8). Untreated specimens were compared with airborne-particle abraded ones. Specimens with 3 mol% yttria were further coated with polyelectrolyte multilayers (n=4). The surfaces were characterized by measuring the roughness, hydrophobicity, and surface charge using profilometry, atomic force microscopy, tensiometry, and electrokinetic analyzer, respectively. The extent of bacterial adhesion was determined using spectrophotometry and scanning electron microscopy. Data were analyzed with a single-factor ANOVA and F-test for variance (α=.05).

Results. The airborne-particle abrasion of zirconia increased the surface roughness, which led to the pronounced adhesion of *Streptococcus mutans*. However, polyelectrolyte multilayer coatings made of chitosan and pol(yacrylic acid) reduced the extent of bacterial adhesion, especially in as-sintered specimens, with 70% fewer adhered bacteria than airborne-particle abraded specimens. The effect of polyelectrolyte multilayer coating on the airborne-particle abraded series was greatest with the poly (acrylic acid)-terminating specimens, with 50% fewer adhered bacteria than the uncoated ones.

Conclusions. Airborne-particle abraded zirconia specimens coated with biocompatible polyelectrolyte multilayer coatings with a negatively charged terminating layer were associated with a 50% reduction in bacteria adhesion compared with uncoated specimens. (J Prosthet Dent 2025;133:1343.e1-e9)

Zirconia stabilized with 3 mol % yttria (3Y-TZP) has become popular for fixed partial dentures (FPDs), monolithic crowns, and implant abutments,[1–5] with excellent mechanical properties associated with the tetragonal-to-monoclinic (*t*→*m*) transformation toughening mechanism.[6–9] However, early zirconia restorations were prone to spontaneous *t*→*m* transformation induced by moisture, often occurring in humid environments and leading to a sharp decrease in mechanical properties and consequent failures.[10–12]

Recently, translucent zirconia ceramics have been introduced with new dopants, increasing the yttria (Y_2O_3) amount to 4 or 5 mol% and reducing the amount of alumina (Al_2O_3) (≤0.1 wt%).[13] These zirconia ceramics have become popular as monolithic crowns, occlusal veneers, or FPDs. The increased yttria content has drawbacks, since it overstabilizes the tetragonal crystal lattice, reducing the *t*→*m* toughening.[14–17] These materials have reduced mechanical properties and an optically isotropic cubic crystal phase, which enhances the

Supported by the Slovenian Research and Innovation Agency (ARIS), Health Protection Mechanisms program (ARIS P3–0388), Slovenia.
No conflict of interest.
[a]Researcher, Department for Nanostructured Materials, Jožef Stefan Institute, Ljubljana, Slovenia.
[b]Graduate student, Faculty of Health Sciences, University of Ljubljana, Ljubljana, Slovenia.
[c]Lecturer, Faculty of Health Sciences, University of Ljubljana, Ljubljana, Slovenia.
[d]Researcher, Faculty of Health Sciences, University of Ljubljana, Ljubljana, Slovenia.
[e]Researcher, Department of Chemistry, Faculty of Science, University of Zagreb, Zagreb, Croatia.
[f]Professor, Department of Chemistry, Faculty of Science, University of Zagreb, Zagreb, Croatia.
[g]Professor, Faculty of Health Sciences, University of Ljubljana, Ljubljana, Slovenia.
[h]Professor, Faculty of Health Sciences, University of Ljubljana, Ljubljana, Slovenia.

Clinical Implications

Airborne-particle abrasion of zirconia is a common practice that alters the surface morphology. The increased tendency to form biofilm on such surfaces must be accounted for and mitigated. The introduction of polyelectrolyte multilayers on the surface of ceramics significantly altered the propagation of biofilms.

translucency by scattering the incident light.[18,19] Appropriate translucent zirconia ceramics can be used for minimally invasive dentistry in the esthetic zone, including for resin-bonded FPDs.[20] Understanding the parameters that govern the strength of the bond between such restorations and tooth structures is crucial.

The properties of the zirconia-resin junction, adhesion, and the aging of zirconia (low-temperature degradation) can be improved with low-pressure airborne-particle abrasion (APA),[21] as it introduces residual compressive stress (causing $t \rightarrow m$ phase transformation) into a subsurface layer a few micrometers thick.[22–24] Whereas most of the APA-treated FPD surface is covered with resin once applied clinically, the margins remain exposed to the surrounding environment.[25] APA leads to an increased effective surface area for bonding, but an increased number of surface defects occur.[22,26] These defects prevent the removal of bacteria and increase the strength of their attachment, which results in a higher rate of adhered bacteria[27] and an increased possibility of developing bacterial biofilms.[28–32] Such films can lead to the demineralization of mineralized tissue or infections of the soft tissues. *Streptococcus mutans* (*S. mutans*) has been identified as a major etiologic factor for caries.[33–36]

The surface properties of dental materials can be improved with the application of coatings. Recently, polyelectrolyte multilayers (PEMs) based on the layer-by-layer build-up have experienced a surge in their applications, including in dentistry.[37–39] PEMs are a stack of alternating polycation and polyanion layers on the surface, commonly prepared by dipping the surface in oppositely charged polyelectrolyte solutions.[40] The build-up of PEMs in a layer-by-layer fashion enables precise control of the thickness, surface roughness, mechanical strength, and wettability of these coatings.[41] In addition, the properties of PEMs can be fine-tuned by the polyelectrolytes used and by adjusting the parameters of PEM preparation.[38] It has been reported that PEMs can improve bacteriostatic properties,[42] as the surface charge is an important parameter that reduces the extent of adhered bacteria on the surface. Bacterial adhesion has been reported to be higher on positively charged rather than negatively charged surfaces since most bacterial cells are negatively charged and thus repulsed by negatively charged surfaces.[43–45]

This study aimed to evaluate how different zirconia ceramic compositions and various surface treatments, including PEM coatings, affect *S. mutans* adhesion and consequent biofilm formation. Formation of the biofilm is a complex process that is influenced by various factors, including material surface characteristics, environmental factors, and bacterial properties.[46–49] A better understanding of these factors is needed to control bacterial adhesion.[43,50] Therefore, the surface properties of charge density, roughness, and hydrophobicity were studied, and their influence on the extent of *S. mutans* adhesion to the surfaces was investigated. The research hypothesis was that PEM coatings composed of chitosan (CS) and poly(acrylic acid) (PAA) could significantly inhibit bacterial adhesion to abraded zirconia.

MATERIAL AND METHODS

Zirconia ceramics with additives were prepared as shown in Table 1. Ceramic powder (m=1.8 ±0.01 g) was isostatically pressed into Ø20-mm disks at 150 MPa. The disks were first sintered at 1000 °C for 1 hour, followed by another step at 1450 °C for 2 hours and left in the furnace until the temperature reached 40 °C and the diameter of the fully sintered ceramic disks was 16 mm. Half of the disks were left untreated (as-sintered, AS), and the other half were airborne-particle abraded (APA) with 50-μm aluminum oxide. The specimens were cleaned in distilled water and 96% ethanol.

PEMs were prepared on the zirconia substrates using the layer-by-layer method[51] with solutions of PAA (Sigma-Aldrich) (M_w≈1800 g/mol) and CS (Sigma-Aldrich) (medium molecular weight). While the mass concentration of polymers in both solutions was the same (γ=4 g/L), the pH of the PAA solution was 2.8, and that of the CS solution was 3.0. The pH of the polyelectrolyte solutions was adjusted with 1.0 M acetic acid solution (Chem-Lab NV) using a pH-meter (826 pH mobile; Metrohm) equipped with a combined glass microelectrode (The substrates were first immersed for 15 minutes in PAA solution, then immersed in deionized water once for 3 minutes and twice for 1 minute, and then dried with argon or nitrogen (Messer). After drying, the PAA-coated substrates were dipped for 15

Table 1. Zirconium oxide ceramics with additives and their chemical composition produced by TOSOH (Tokyo, Japan)

Specimen Name	Commercial Powder	Composition
3Y-T	TZ-PX–242A	ZrO_2 + 3 mol% Y_2O_3 + 0.05 wt% Al_2O_3
3Y	TZ- 3YB-E	ZrO_2 + 3 mol% Y_2O_3 + 0.25 wt% Al_2O_3
4Y	Zpex 4	ZrO_2 + 4 mol% Y_2O_3 + 0.05 wt% Al_2O_3
5Y	Zpex Smile	ZrO_2 + 5.2 mol% Y_2O_3 + 0.05 wt% Al_2O_3

minutes in a CS solution and then rinsed and dried as described previously. The process was repeated for several cycles to yield a 6- and 7-layer coating. Prepared PEMs were designated as $(PAA/CS)_3$ when the last layer was positively charged chitosan and $(PAA/CS)_3$-PAA when the last layer was negatively charged poly(acrylic acid).

Surface roughness was measured with a mechanical profilometer (Form Talysurf Series 2; Taylor-Hobson). According to the International Organization for Standardization (ISO) 21920–2:2021 standard,[52] a 0.8-mm Gaussian filter was applied to differentiate between the waviness and roughness of the surface.

The zeta potentials of the material surfaces were measured with an electrokinetic analyzer (SurPASS; Anton Paar) at room temperature in 10-mM phosphate-buffered saline (PBS) in a solution at 7.5 pH. The measured streaming potential values were used for the calculation of zeta potential values by means of the Helmholtz-Smoluchowski equation.[53,54]

An optical tensiometer (Attension Theta; Biolin Scientific) was used to measure the static contact angle between 5-μL drops of distilled water and the specimen in 5 repetitions. The data were analyzed using the Young-Laplace equation in a software program (OneAttension version 3.2: Biolin Scientific).[55] Measurements were performed at 24 ±2 °C and 35 to 50% relative humidity.

The PEM surface topography and roughness at the nanoscale were investigated by means of a tapping mode (NCHV-A probe; Bruker) atomic force microscope (AFM MultiMode8; Bruker). For the local root mean square (RMS) roughness determination, surface images were made at 5 different locations on the specimen. Images were later corrected for tilt and bow by using a second order flatten fit. Finally, average values and corresponding standard errors were calculated. Analysis programs (NanoScope 9.7 and NanoScope Analysis 2.0; Bruker Corp) were used to process the measurements and analyze the obtained data.

The *S. mutans* ATCC 25175 standard strains were used in the study, as it has been the most associated with plaque formation[56,57] and the adhesion of *S. mutans* has been reported to lead to dental caries and periodontitis.[33–36] The bacteria were cultured on blood agar plates in an atmosphere augmented with CO_2 for 24 hours at 37 °C. The overnight culture was prepared in 5 mL of brain-heart infusion (BHI) nutrient broth (4012302; Biolife Italiana Srl) for 18 hours at 37 °C.

Before the assay, the specimens were sterilized with UV (G30W T8; Sylvania). The specimens were incubated with a diluted (1:30) overnight culture of *S. mutans* in BHI broth for 24 hours at 37 °C in 6-well culture plates. The negative control was incubated with sterilized BHI. After incubation, the specimens were washed with 1 M PBS and air dried using hot air. Two methods were used to evaluate bacterial adhesion: crystal violet (CV) assay and scanning electron microscopy (SEM).

To determine the extent of the bacterial adhesion using a spectrophotometer (Infinite 200 PRO; Tecan Group Ltd.), the biofilm was stained with a 0.4% crystal violet stain (CV) (115940; Merck) solution and incubated for 5 minutes. Excess dye was removed using 1 M PBS solution, and the bound CV was extracted by incubating it with 96% ethanol for 5 minutes. Then, 200 μL of the ethanol-CV mixture was transferred to a microtiter plate. The amount of biofilm was measured at an optical density of 620 nm. The CV bound to the negative control was subtracted from the mean value.

For SEM analysis, the specimens were washed with PBS and distilled water and dried with hot air. Before imaging, a 7-nm gold layer was deposited on the surface using a precision etching coating system (Model 682; Gatan, Inc) system to achieve a conductive specimen. Bacterial adhesion was assessed using a scanning electron microscope (JSM-7600F; JEOL, Ltd.) in SE mode at 5 keV. For the quantitative analysis of adhered bacteria, a software package (ImageJ, Version 1.50b; National Institutes of Health) was used to count the adhered bacteria.

Statistical analyses were carried out in a statistical software program (Excel 2108 Build 14332.20791 with Analysis ToolPak Add-in package; Microsoft Corp). Data were analyzed with a single-factor ANOVA and F-test for variance (α=.05).

RESULTS

Figure 1 represents the RMS roughness of substrates without PEMs, as measured by profilometry. The

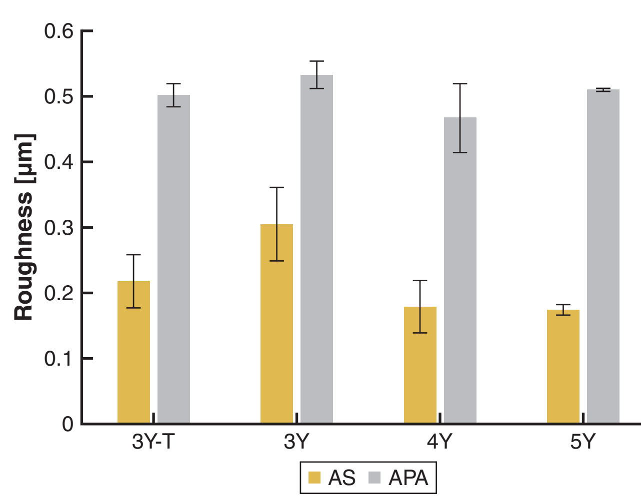

Figure 1. Root mean square roughness of AS and APA surfaces determined by profilometry. APA, airborne-particle abrasion; AS, as-sintered.

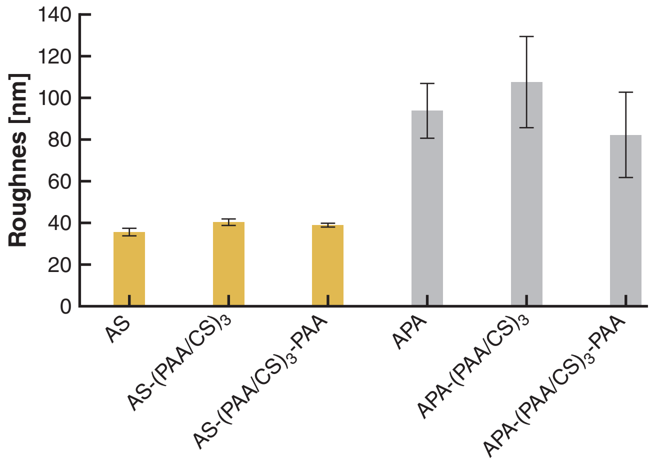

Figure 2. Root mean square roughness of unmodified 3Y AS and 3Y APA surfaces and the same surfaces modified with $(PAA/CS)_3$ and $(PAA/CS)_3$-PAA multilayers as determined by AFM. AFM, atomic force microscopy; APA, airborne-particle abrasion; AS, as-sintered; CS, chitosan; PAA, poly(acrylic acid).

highest roughness (from 0.47 to 0.53 µm) was measured on APA surfaces, approximately double the roughness of AS materials. PEMs have a thickness in the nanometer range, and, therefore, AFM was used to measure the local roughness. Figure 2 shows the roughness parameter for 3Y AS and 3Y APA surfaces before and after coating the substrate surface with $(PAA/CS)_3$ and $(PAA/CS)_3$-PAA multilayers. The AFM measurements confirmed the profilometry results that the 3Y APA specimen has higher roughness than the 3Y AS specimen ($P<.05$). However, the surface roughness of both substrates did not change significantly within the group after PEM formation ($P>.05$).

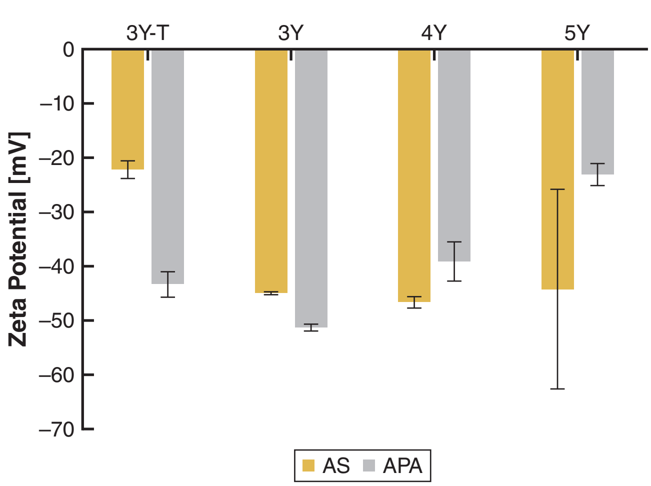

Figure 3. Zeta potentials of AS and APA surfaces in 0.01 M PBS solution at pH=7.5 and room temperature. APA, airborne-particle abrasion; AS, as-sintered; PBS, phosphate-buffered saline.

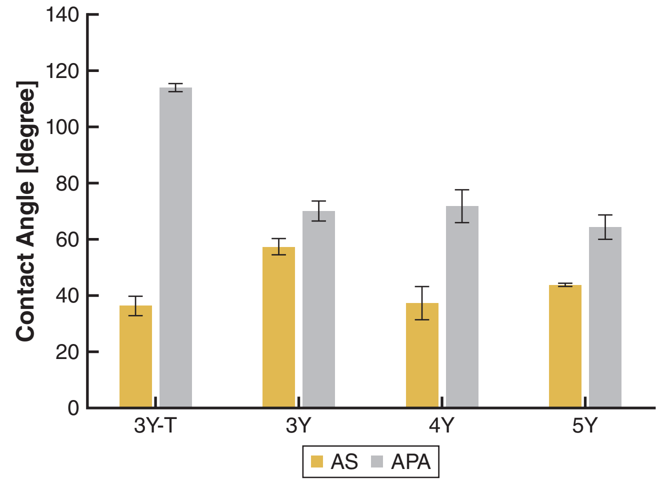

Figure 4. Contact angle of water droplets (V=5 µL) on AS and APA surfaces. APA, airborne-particle abrasion; AS, as-sintered.

As presented in Figure 3, the results obtained by the zeta potential measurements showed that all investigated surfaces were negatively charged in 0.01 M PBS solution at pH=7.5 at room temperature. The lowest zeta potential value was obtained on 3Y APA (–51.3 ±0.6 mV) and the least negative on the 3Y-T AS (–22.2 ±1.6 mV) surfaces ($P<.05$).

Figure 4 shows the contact angles measured with the optical tensiometer. Only the 3Y-T APA surface was hydrophobic, with a contact angle of 114 degrees. Other surfaces were hydrophilic with a contact angle lower than 72 degrees. The lowest contact angle was on 4Y AS (37 degrees) ($P<.05$). The APA surfaces, in general, exhibited larger contact angles than the AS surfaces.

PEM coatings significantly changed the contact angle of the surface, with an increasing number of adsorbed polyelectrolyte layers ($P<.05$) (Fig. 5). The contact angle systematically alternated from less hydrophilic to more hydrophilic values as the terminating layer was changed from PAA to CS. This kind of zigzag dependence of the contact angle on the number of deposited polyelectrolyte layers indicates a successful PEM build-up.[41]

Figure 6 shows the morphological changes on the AFM images of 3Y AS and 3Y APA surfaces before and after coating the surface with 6 and 7 adsorbed polyelectrolyte layers of PEM. The most significant surface changes were observed for 3Y AS coated with the PAA/CS_3 multilayer.

Figure 7 shows the extent of bacterial adhesion on the AS and APA surfaces with different compositions. After 24-hour incubation, there was a general trend towards an increase in the absorbance for APA compared with AS surfaces. The lowest absorbance was on the 4Y AS (0.12 ±0.03), and the highest on the 3Y-T AS

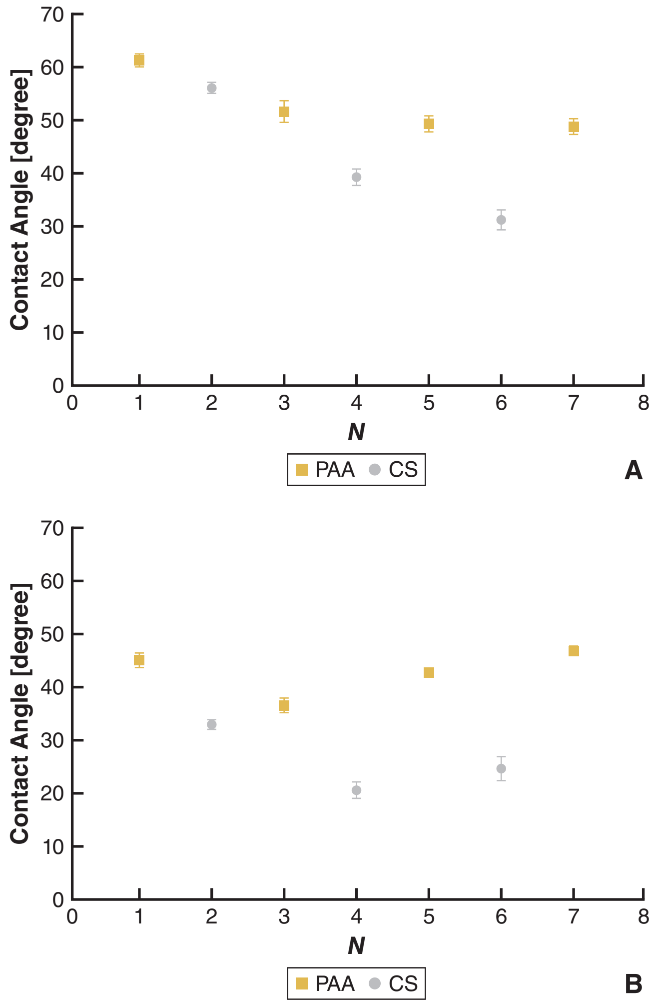

Figure 5. Evolution of water contact angles during build-up of PAA/CS multilayers on surface of 3Y AS (A) and 3Y APA (B) substrate. Odd layer numbers *N* represent films with PAA as terminating layer, whereas even layer numbers *N* represent films with CS as terminating layer. APA, airborne-particle abrasion; AS, as-sintered; CS, chitosan; PAA, poly (acrylic acid).

(0.38 ±0.04). Increased yttria content was not associated with a significant difference (P>.05).

Figure 8 shows micrographs of *S. mutans* adhered to the AS and APA 5Y zirconia surfaces. The chains of *S. mutans* are observed on the AS surface. The APA surfaces had higher roughness and were nonhomogeneous. The adhered bacteria used the surface features as preferential adhesion regions, indicating that the formation of the film was morphologically driven.

Bacterial adhesion on PEM-coated specimens was evaluated using SEM micrographs. Traditional optical staining methods were not suitable because of the simultaneous staining of PEMs. A quantitative analysis of adhered bacteria using the encircling method is shown in Figures 9 and 10.

DISCUSSION

In this study, the impact of surface roughness, wettability, zeta potential, and PEM coatings on the extent of bacterial adhesion was analyzed. The research confirmed the hypothesis that PEM coatings composed of chitosan (CS) and poly(acrylic acid) (PAA) can significantly inhibit bacterial adhesion to abraded zirconia. The surface roughness of zirconia specimens has been measured on 2 scales: on the micrometer scale with profilometry, which offers an insight into coarser features (Fig. 1) and at the nanoscale with AFM (Fig. 2). Both methods show a similar trend, with APA specimens being approximately twice as rough as AS ones. The degree of *S. mutans* biofilm formation observed over a time period of 24 hours (Fig. 7) demonstrated a positive correlation between surface roughness and the amount of biofilm accumulation, consistent with previous studies.[28–31,36] The same has also been reported for the following bacteria: *Escherichia coli*, *Staphylococcus aureus*, and *Pseudomonas aeruginosa*.[27] However, a weak correlation has also been reported between bacterial adhesion and surface roughness.[32,34]

Wettability, which depends on material and bacteria, also plays a significant role in the initial phase of bacterial adhesion.[48] *S. mutans* has been reported to be more hydrophobic compared with other bacteria.[47,49] A general rule is that the antibacterial properties of the surface improve if the contact angle of the surface decreases.[46] The present study indicates that more hydrophilic AS surfaces have lower bacterial adhesion extent than APA surfaces (with the exception of 3Y-T specimens).

Surface charge also has a significant effect on bacterial adhesion.[42] All the tested ceramic materials were negatively charged at the physiological pH (pH=7.5). The least negative charge was measured on the surfaces of 3Y-T AS and 5Y APA (Fig. 3). Those surfaces exhibited the highest extent of bacterial adhesion (Fig. 7). Therefore, keeping the surface charge low was found to reduce biofilm formation, consistent with other studies.[43–45,58]

The beneficial properties of PEMs were most clearly observed in AS specimens compared with the control (uncoated) specimens. The same was not true for the APA specimens, where the number of bacteria was still lower compared with the non-APA control specimens, but the difference within the APA group was minimal. Rougher surfaces have been reported to host more bacteria.[27] The same surface asperities that shield the biofilm in the cracks and crevices most likely limit growth on more exposed parts. There seems to be a steric interplay between surface roughness and bacterial adhesion that limits the high biofilm growth, as is seen

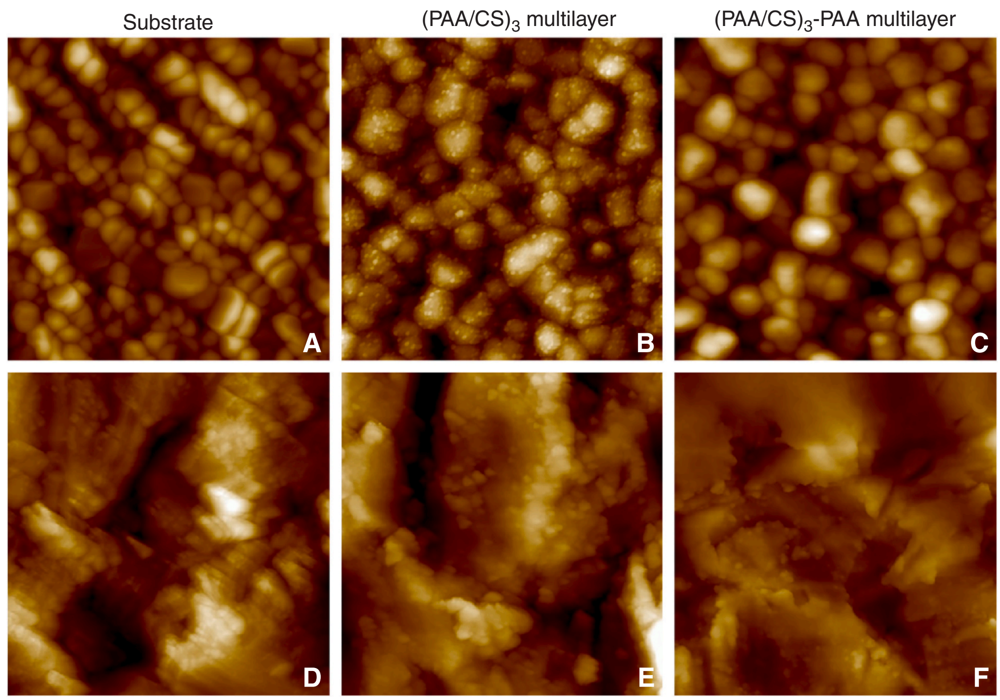

Figure 6. AFM images (5×5 µm^2) of 3Y AS and 3Y APA surface before (A, D) and after (B, C, E, F) coating substrate surface with PAA/CS multilayers. The z-scale is 250 nm on images A-C and 500 nm on images D-F. AFM, atomic force microscopy; APA, airborne-particle abrasion; AS, as-sintered; CS, chitosan; PAA, poly(acrylic acid).

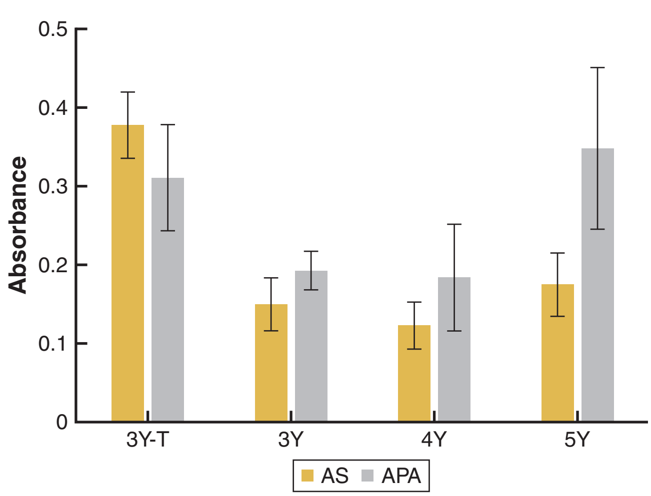

Figure 7. Absorbance of CV for AS and APA surfaces after 24 h incubation in culture of *S. mutans*. APA, airborne-particle abrasion; AS, as-sintered; CV, crystal violet.

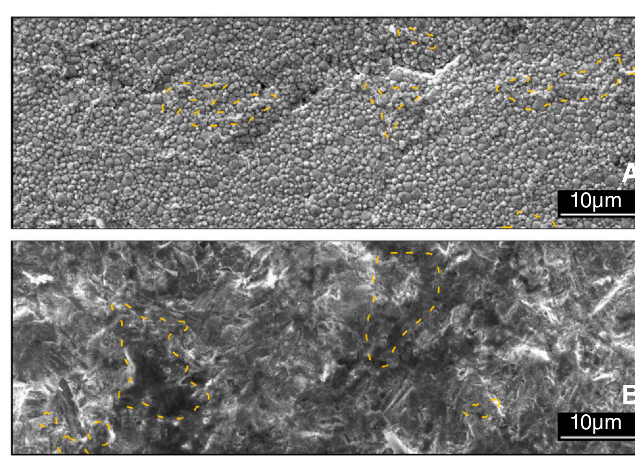

Figure 8. Micrographs with adhered S. mutans on 5Y zirconia surfaces after 24 h of incubation (original magnification ×5000). (a) AS surface, (b) APA surface. APA, airborne-particle abrasion; AS, as-sintered.

in Figure 8. Because of their structure, the encircling method on SEM micrographs for APA surfaces cannot be fully applied and the Z-contrast imaging from backscattered electron micrographs was less reliable for AS surfaces. Limitations of the study included that the impact of PEM coatings on osseointegration should be assessed with live/dead cell tests before moving to in vivo testing, since it is a crucial step in the successful adaptation of the implant. Furthermore, the PEMs could be considered a suitable delivery matrix for introducing nanoparticles that could further inhibit bacterial adhesion and growth. Future work should encompass the application of PEMs to a whole range of zirconia ceramics (with various yttria contents) to serve as the basis for clinical trials.

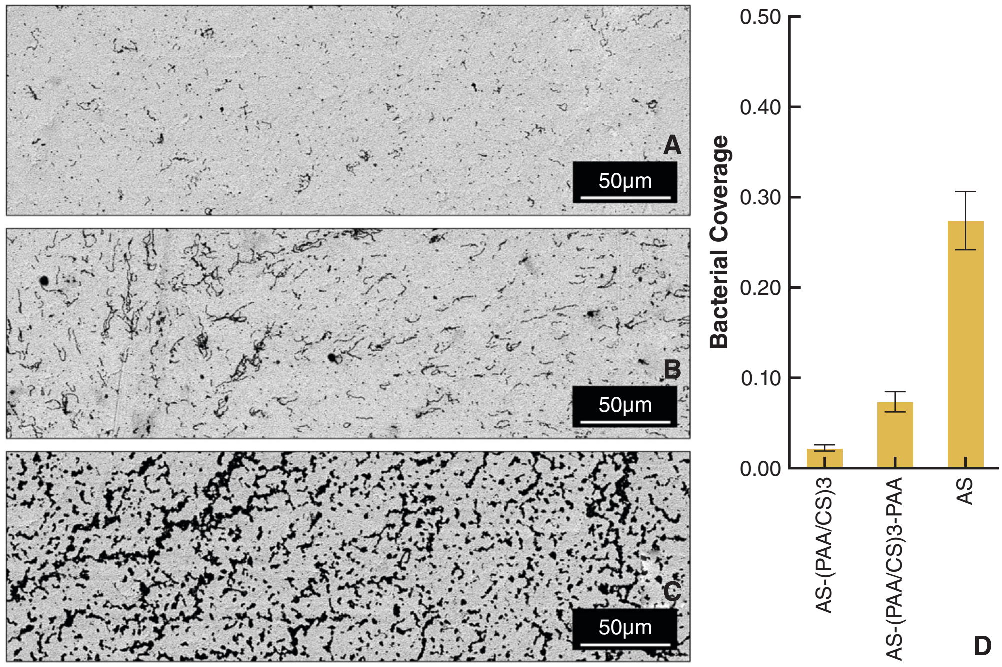

Figure 9. SEM images in the back-scattered mode of 3Y AS (A, B, C) surfaces after coating the substrate surface with 6 (A) and 7 PAA/CS (B) layers. AS specimen without any additional coating (true as-sintered) shown in C and the corresponding bacterial adhesion quantification from SEM micrographs in D. AS, as-sintered; CS, chitosan; PAA, poly(acrylic acid); SEM scanning electron microscope.

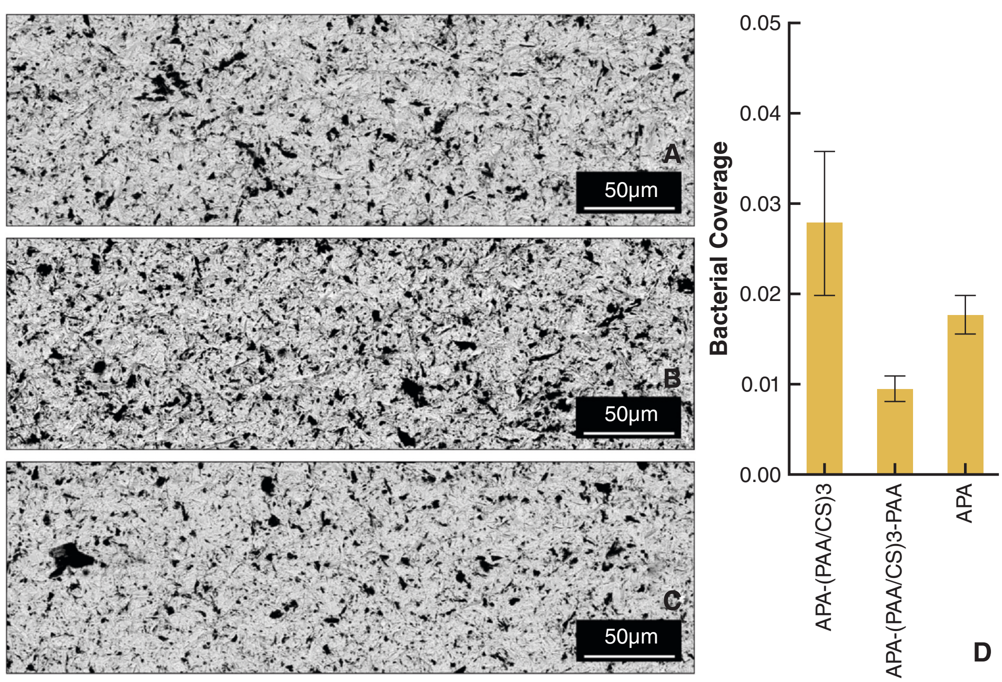

Figure 10. SEM image in the back-scattered mode of 3Y APA (A, B, C) surfaces after coating substrate surface with 6 (A) and 7 PAA/CS (B) layers. Fig. C corresponds to a pure APA surface. The corresponding bacterial adhesion quantification from SEM micrographs is shown in Figure D. APA, airborne-particle abrasion; CS, chitosan; PAA, poly(acrylic acid); SEM scanning electron microscope.

CONCLUSIONS

Based on the findings of this in vitro study, the following conclusions were drawn:

1. Airborne-particle abrasion of Y-TZP bioceramics increased its surface roughness, leading to higher bacterial adhesion on those surfaces.
2. The introduction of PEMs on the surface of ceramics changed the dynamics of biofilm propagation.
3. The inhibition of biofilm growth resulting from lower initial adhesion outweighed the roughening effects from airborne-particle abrasion.
4. A more negative zeta potential led to a lower degree of adhesion of *S. mutans*.
5. PEMs, composed of biocompatible chitosan and poly(acrylic acid), are a suitable option for application in the dental sector, especially on airborne-particle abraded surfaces where they offer a 50% reduction in bacteria adhesion compared with uncoated specimens.

REFERENCES

1. Guess PC, Schultheis S, Bonfante EA, Coelho PG, Ferencz JL, Silva NRFA. All-ceramic systems: Laboratory and clinical performance. *Dent Clin North Am*. 2011;55:333–352.
2. Oblak Č, Jevnikar P, Kosmač T. Properties and clinical application of zirconia bioceramics in medicine. *TEST - Zdrav Vestn*. 2013;82.
3. Madfa AA, Al-Sanabani FA, Al-Qudami NH, Al-Sanabani JS, Amran AG. Use of zirconia in dentistry: An overview. *Open Biomater J*. 2014;5:1–7.
4. Malkondu Ö, Tinastepe N, Akan E, Kazazoğlu E. An overview of monolithic zirconia in dentistry. *Biotechnol Biotechnol Equip*. 2016;30:644–652.
5. Mirt T, Abram A, van del Velde N, et al. Effect of airborne-particle abrasion of yttria-containing zirconia dental ceramics on mechanical properties before and after regeneration firing. *J Eur Ceram Soc*. 2022;42:5035–5044.
6. Hannink RHJ, Kelly PM, Muddle BC. Transformation toughening in zirconia-containing ceramics. *J Am Ceram Soc*. 2004;83:461–487.
7. Kelly J, Denry I. Stabilized zirconia as a structural ceramic: An overview. *Dent Mater*. 2008;24:289–298.
8. Miyazaki T, Nakamura T, Matsumura H, Ban S, Kobayashi T. Current status of zirconia restoration. *J Prosthodont Res*. 2013;57:236–261.
9. Garvie RC, Hannink RH, Pascoe RT. Ceramic steel? *Nature*. 1975;258:703–704.
10. Camposilvan E, Leone R, Gremillard L, et al. Aging resistance, mechanical properties and translucency of different yttria-stabilized zirconia ceramics for monolithic dental crown applications. *Dent Mater*. 2018;34:879–890.
11. Kocjan A, Cotič J, Kosmač T, Jevnikar P. In vivo aging of zirconia dental ceramics – Part I: Biomedical grade 3Y-TZP. *Dent Mater*. 2021;37:443–453.
12. Cotič J, Kocjan A, Panchevska S, Kosmač T, Jevnikar P. In vivo ageing of zirconia dental ceramics — Part II: Highly-translucent and rapid-sintered 3Y-TZP. *Dent Mater*. 2021;37:454–463.
13. Güth JF, Stawarczyk B, Edelhoff D, Liebermann A. Zirconia and its novel compositions: What do clinicians need to know? *Quintessence Int*. 2019;50:512–520.
14. Zhang F, Reveron H, Spies BC, Van Meerbeek B, Chevalier J. Trade-off between fracture resistance and translucency of zirconia and lithium-disilicate glass ceramics for monolithic restorations. *Acta Biomater*. 2019;91:24–34.
15. Kwon SJ, Lawson NC, McLaren EE, Nejat AH, Burgess JO. Comparison of the mechanical properties of translucent zirconia and lithium disilicate. *J Prosthet Dent*. 2018;120:132–137.
16. Inokoshi M, Shimizu H, Nozaki K, et al. Crystallographic and morphological analysis of sandblasted highly translucent dental zirconia. *Dent Mater*. 2018;34:508–518.
17. McLaren EA, Lawson N, Choi J, Kang J, Trujillo C. New High-Translucent cubic-phase–containing zirconia: Clinical and laboratory considerations and the effect of air abrasion on strength. *Compend Contin Educ Dent*. 2017;38:e13–e16.
18. Mirt T, Kocjan A, Hofer AK, et al. Effect of airborne particle abrasion and regeneration firing on the strength of 3D-printed 3Y and 5Y zirconia ceramics. *Dent Mater*. 2024;40:111–117.
19. De Araújo-Júnior ENS, Bergamo ETP, Bastos TMC, et al. Ultra-translucent zirconia processing and aging effect on microstructural, optical, and mechanical properties. *Dent Mater*. 2022;38:587–600.
20. Malgaj T, Plut A, Eberlinc A, Drevenšek M, Jevnikar P. Anterior esthetic rehabilitation of an alveolar cleft using novel minimally invasive prosthodontic techniques: A case report. *Cleft Palate Craniofac J*. 2021;58:912–918.
21. Kern M, Wegner SM. Bonding to zirconia ceramic: Adhesion methods and their durability. *Dent Mater*. 1998;14:64–71.
22. Kosmač T, Oblak C, Jevnikar P, Funduk N, Marion L. The effect of surface grinding and sandblasting on flexural strength and reliability of Y-TZP zirconia ceramic. *Dent Mater*. 1999;15:426–433.
23. Yoshida K. Influence of alumina air-abrasion for highly translucent partially stabilized zirconia on flexural strength, surface properties, and bond strength of resin cement. *J Appl Oral Sci*. 2020;28:e20190371.
24. Cotič J, Jevnikar P, Kocjan A. Ageing kinetics and strength of airborne-particle abraded 3Y-TZP ceramics. *Dent Mater*. 2017;33:847–856.
25. Walmsley AD, Walsh TF, Lumley P, et al. The principles of tooth replacement. Restorative Dentistry. 2nd ed..,. Elsevier,; 2007:145–196.
26. Ramos-Tonello CM, Trevizo BF, Rodrigues RF, et al. Pre-sintered Y-TZP sandblasting: effect on surface roughness, phase transformation, and Y-TZP/veneer bond strength. *J Appl Oral Sci*. 2017;25:666–673.
27. Bohinc K, Dražić G, Fink R, et al. Available surface dictates microbial adhesion capacity. *Int J Adhes Adhes*. 2014;50:265–272.
28. Busscher HJ, Rinastiti M, Siswomihardjo W, van der Mei HC. Biofilm formation on dental restorative and implant. *Materials (Basel). J Dent Res*. 2010;89:657–665.
29. Vo DT, Arola D, Romberg E, Driscoll CF, Jabra-Rizk MA, Masri R. Adherence of Streptococcus mutans on lithium disilicate porcelain specimens. *J Prosthet Dent*. 2015;114:696–701.
30. Aykent F, Yondem I, Ozyesil AG, Gunal SK, Avunduk MC, Ozkan S. Effect of different finishing techniques for restorative materials on surface roughness and bacterial adhesion. *J Prosthet Dent*. 2010;103:221–227.
31. Kawai K, Urano M, Ebisu S. Effect of surface roughness of porcelain on adhesion of bacteria and their synthesizing glucans. *J Prosthet Dent*. 2000;83:664–667.
32. Buergers R, Rosentritt M, Handel G. Bacterial adhesion of Streptococcus mutans to provisional fixed prosthodontic material. *J Prosthet Dent*. 2007;98:461–469.
33. Bislimi F, Bajevska J, Garai M, Reka AA. A study on the bacterial adhesion of Streptococcus mutans in various dental ceramics: In vitro study. *Open Chem*. 2020;18:1334–1338.
34. Chenicheri S, R U, Ramachandran R, Thomas V, Wood A. Insight into oral biofilm: Primary, secondary and residual caries and phyto-challenged solutions. *Open Dent J*. 2017;11:312–333.
35. Ichikawa Hirota, Kanitani Miyake, Matsumoto. In vitro adherence of Streptococcus constellatus to dense hydroxyapatite and titanium. *J Oral Rehabil*. 1998;25:125–127.
36. Lee BC, Jung GY, Kim DJ, Han JS. Initial bacterial adhesion on resin, titanium and zirconia in vitro. *J Adv Prosthodont*. 2011;3:81.
37. Sukhishvili SA. Responsive polymer films and capsules via layer-by-layer assembly. *Curr Opin Colloid Interface Sci*. 2005;10:37–44.
38. Dash P, Thirumurugan S, Hu C, Wu C, Shih S, Chung R. Preparation and characterization of polyelectrolyte multilayer coatings on 316L stainless steel for antibacterial and bone regeneration applications. *Surf Coat Technol*. 2022;435:128254.
39. Boonbanyen A, Angwaravong O, Kanjanamekanant K, Angwarawongg T. Adlay polyelectrolyte multilayer films coated on titanium: Surface characteristics and MC3T3-E1 cell morphology and proliferation. *J Health Sci Med Res JHSMR*. 2024;42:e2023987.
40. Decher G. Fuzzy Nanoassemblies: Toward layered polymeric multicomposites. *Science*. 1997;277:1232–1237.
41. Elzbieciak M, Kolasinska M, Warszynski P. Characteristics of polyelectrolyte multilayers: The effect of polyion charge on thickness and wetting properties. *Colloids Surf Physicochem Eng Asp*. 2008;321:258–261.
42. Kovačević D, Pratnekar R, Godič Torkar K, et al. Influence of polyelectrolyte multilayer properties on bacterial adhesion capacity. *Polymers ((Basel))*. 2016;8:345.
43. Katsikogianni M, Missirlis Y. Concise review of mechanisms of bacterial adhesion to biomaterials and of techniques used in estimating bacteria-material interactions. *Eur Cell Mater*. 2004;8:37–57.
44. Song F, Koo H, Ren D. Effects of material properties on bacterial adhesion and biofilm formation. *J Dent Res*. 2015;94:1027–1034.
45. Terada A, Okuyama K, Nishikawa M, Tsuneda S, Hosomi M. The effect of surface charge property on Escherichia coli initial adhesion and subsequent biofilm formation. *Biotechnol Bioeng*. 2012;109:1745–1754.
46. Spriano S, Sarath Chandra V, Cochis A, et al. How do wettability, zeta potential and hydroxylation degree affect the biological response of biomaterials? *Mater Sci Eng C*. 2017;74:542–555.

47. Quirynen M, Bollen CML. The influence of surface roughness and surface-free energy on supra- and subgingival plaque formation in man: A review of the literature. *J Clin Periodontol*. 2005;22:1–14.
48. Azam M, Khan A, Muzzafar D, et al. Structural, surface, in vitro bacterial adhesion and biofilm formation analysis of three dental restorative composites. *Materials ((Basel))*. 2015;8:3221–3237.
49. Harris JM, Martin LF. An In vitro study of the properties influencing Staphylococcus epidermidis adhesion to prosthetic vascular graft materials. *Ann Surg*. 1987;208:612–620.
50. An YH, Friedman RJ. Concise review of mechanisms of bacterial adhesion to biomaterial surfaces. *J Biomed Mater Res*. 1998;43:338–348.
51. Decher G, Hong JD, Schmitt J. Buildup of ultrathin multilayer films by a self-assembly process: III. Consecutively alternating adsorption of anionic and cationic polyelectrolytes on charged surfaces. *Thin Solid Films*. 1992;210–211:831–835.
52. International Organization for Standardization. Geometrical product specifications (GPS) - Surface texture: Profile Part 2: Terms, definitions and surface texture parameters. Geneva, Switzerland; 2021.
53. Nishimura S, Yao K, Kodama M, Imai Y, Ogino K, Mishima K. Electrokinetc study of synthetic smectites by flat plate streaming potential technique. *Langmuir*. 2002;18:188–193.
54. Bukšek H, Luxbacher T, Petrinić I. Zeta potential determination of polymeric materials using two differently designed measuring cells of an electrokinetic analyzer. *Acta Chim Slov*. 2010;57:700–706.
55. Río OI del, Neumann AW. Axisymmetric drop shape analysis: Computational methods for the measurement of interfacial properties from the shape and dimensions of pendant and sessile drops. *J Colloid Interface Sci*. 1997;196:136–147.
56. Valm AM. The structure of dental plaquemicrobial communities in the transition from healthto dental caries and periodontal disease. *J Mol Biol*. 2019;431:2957–2969.
57. Vinogradov AM, Winston M, Rupp CJ, Stoodley P. Rheology of biofilms formed from the dental plaque pathogen. *Biofilms*. 2004;1:49–56.
58. Kreve S, dos Reis AC. Effect of surface properties of ceramic materials on bacterial adhesion: A systematic review. *J Esthet Restor Dent*. 2022;34:461–472.

Corresponding author:
Prof Klemen Bohinc
Faculty of Health Sciences
University of Ljubljana
Ljubljana 1000
SLOVENIA
Email: klemen.bohinc@zf.uni-lj.si

https://doi.org/10.1016/j.prosdent.2025.01.038